

## Ultrathin films of cobalt on Fe{001} and the effect of oxygen

S. K. Kim, C. Petersen, F. Jona, and P. M. Marcus

*Department of Materials Science and Engineering, State University of New York at Stony Brook, Stony Brook, New York 11794-2275*

(Received 29 December 1995; revised manuscript received 5 March 1996)

Deposition of Co on a clean Fe{001} surface in ultrahigh vacuum yields initially films with  $1\times 1$  low-energy electron-diffraction (LEED) patterns up to thicknesses of about 15 Å, then films with increasingly high-background  $c(2\times 2)$  LEED patterns for thicknesses up to about 30 Å, and finally disordered films for larger thicknesses. Quantitative LEED analysis finds the  $1\times 1$  films to have a body-centered-tetragonal structure with in-plane lattice constant  $a=2.87$  Å (pseudomorphic with the Fe{001} substrate) and  $c=2.792$  Å; the first interlayer spacing is contracted by about 11%. Strain analysis of the bulk identifies this structure as a tetragonal distortion of metastable bcc Co. The  $c(2\times 2)$  films are found to be pseudomorphic distortions of hcp Co( $11\bar{2}0$ ), which has a rectangular unit mesh that requires a 6.6% compression in one and a 0.4% compression in the other direction in the surface plane; the film has a bulk interlayer spacing of 1.29 Å (expanded 2.9% over the equilibrium value 1.2535 Å) and about 10% contraction of the first interlayer spacing. It was found that a monolayer of oxygen chemisorbed on the Fe{001} surface before deposition of Co extends the stability range of the strained bcc phase considerably. The oxygen “floats” on the surface of the Co film and a 30-Å film still has the  $1\times 1$  distorted bcc structure, but with a monolayer of oxygen on top. Thicker Co films no longer produce measurable LEED patterns, so that the onset of the  $c(2\times 2)$ -distorted hcp ( $11\bar{2}0$ ) structure cannot be observed. [S0163-1829(96)09127-8]

### I. INTRODUCTION

This paper describes a quantitative study of the epitaxial growth of ultrathin films of Co on single-crystal Fe{001} substrates. Interest in this heteroepitaxial system has both scientific and technological origins, the former because it is expected that epitaxy may stabilize the metastable body-centered-cubic (bcc) phase of Co, the latter because structures involving alternating magnetic layers exhibit enhanced magnetic properties.

Li and Tonner<sup>1</sup> showed, by means of measurements of the angular distributions of x-ray-excited photoemission and Auger electrons, that an ultrathin (three-layer) film of Co grown on top of an ultrathin (3.5-layer) film of bcc Fe, itself on top of Ag{001}, had the bcc structure. Subsequent work by Zhang *et al.*<sup>2</sup> with x-ray photoelectron diffraction (XPD) showed that Co films grown on single-crystal Fe{001} substrates and with thicknesses ranging up to about 20 Å had the bcc structure. One expects that in order to stabilize the metastable bcc phase the epitaxy would have to be pseudomorphic, in which case the Co films would generally be strained away from the ideal bcc structure, but neither of these studies<sup>1,2</sup> observed or reported noncubic distortions of the epitaxial Co films.

Houdy *et al.*<sup>3</sup> grew a series of Fe/Co multilayers (on Si{111}) with different thicknesses of Co and Fe and characterized their structures by ellipsometry, x-ray diffraction (XRD), Auger profile analysis, and transmission electron microscopy. They found that the Co layers had the bcc structure for thicknesses smaller than 20 Å and “a mixed fcc-hcp phase” for thicknesses larger than 20 Å (up to 100 Å).

All the above-mentioned studies are in agreement with one another in reaching the conclusion that ultrathin films of Co grown on Fe substrates have the bcc structure. The evidence for this conclusion was in all cases the comparison

between (XPD or XRD) curves from the Co film, on one hand, and equivalent curves from the Fe substrate, on the other. None of those studies, however, reported quantitative determinations of the atomic structure (i.e., interatomic distances) or of the strains that are expected to exist in the Co films if indeed they grow pseudomorphically on the Fe substrate.

The present work was done precisely for the purpose of determining both the structure and the strains in ultrathin films of Co grown epitaxially on single-crystal Fe{001} substrates and to prove that the structure was in fact strained bcc. The experimental tools used for this purpose were quantitative low-energy electron diffraction (QLEED) and Auger electron spectroscopy (AES). We describe, in Sec. II, the experiments; in Sec. III, the QLEED analysis; in Sec. IV, the strain analysis; in Sec. V, an interesting effect of oxygen on the growth of the Co films; and in Sec. VI, the conclusions.

### II. EXPERIMENTS

The experiments were done in an ultrahigh-vacuum chamber capable of reaching a base pressure of about  $1\times 10^{-10}$  Torr and provided with front-view low-energy electron-diffraction (LEED) optics both for crystallographic studies and, in the retarding-field analyzer mode, for AES measurements. The Fe{001} substrate was a small platelet with approximate size  $6\times 6\times 0.5$  mm<sup>3</sup>. In the experimental chamber the Fe sample could be heated either by radiation or by electron bombardment on the back surface. Its temperature was measured by means of an infrared radiometer with an accuracy estimated at  $\pm 50$  °C. The LEED intensity data needed for quantitative structure analysis [the so-called  $I(V)$  curves] were measured with a video-LEED system described elsewhere.<sup>4</sup>

The sample surface was cleaned *in situ* by a series of

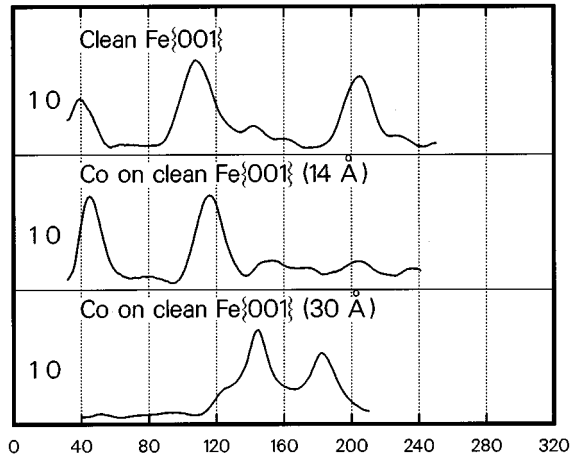


FIG. 1. Ten normal-incidence experimental LEED spectra from clean Fe{001} (top), a 14-Å film of Co grown on Fe{001} (middle), and a 30-Å film of Co grown of Fe{001} (bottom). The 14-Å film obviously had a structure similar to that of Fe{001}, but with a contracted interlayer spacing, whereas the 30-Å film had a different structure.

Ar-ion bombardments (about  $2 \times 10^{-5}$  Torr, 375 eV,  $0.3 \mu\text{A}/\text{cm}^2$ ) and high-temperature anneals (about  $700^\circ\text{C}$  for 1–2 h) and its chemical state was monitored by AES. The Co source consisted of a 1-mm-diam, 99.9%-pure Co wire tightly wound on a tungsten spiral that could be electrically heated. During deposition of Co on the substrate surface the tungsten spiral was heated to temperatures between  $1050^\circ\text{C}$  and  $1250^\circ\text{C}$ . The deposition rates were kept slow at approximately  $1 \text{ \AA}/\text{min}$  or lower. During deposition the substrate was neither heated nor cooled: its temperature was monitored with an infrared pyrometer and was never at or above the minimum temperature measurable with this instrument ( $\sim 150^\circ\text{C}$ ). Previous experiments using identical sources and a thermocouple showed that the substrate was not significantly heated by radiation from the source during deposition. The thickness of the Co films was estimated from the decrease of the Fe AES signal and the increase of the Co AES signal, as described elsewhere (see, e.g., Ref. 5).

Upon deposition of Co, the LEED pattern from the clean Fe{001} surface, a fourfold-symmetric, high-contrast, low-background pattern, persisted as  $1 \times 1$ , with slow but progressive increase of the background and broadening of the diffracted beams, up to Co thicknesses of about  $15 \text{ \AA}$ . The  $I(V)$  curves from the Co film remained similar to those from the Fe substrate, but all peaks appeared shifted toward higher electron energies, as shown for the 10 spectra from clean Fe{001} and a 14-Å Co film in the top two panels of Fig. 1. Both the similarity and the shifts indicate that the Co film had a structure similar to that of the substrate, but with smaller interlayer spacing (as would be expected for pseudomorphic growth of a bcc Co film with a unit mesh smaller than that of the substrate). Figure 1 demonstrates that experimental LEED  $I(V)$  curves can provide significant semi-quantitative information even without model calculations.

With prolonged Co deposition the background of the LEED pattern increased considerably, but still allowed the observation of broad half-order beams in a  $c(2 \times 2)$  pattern. The integral-order  $I(V)$  curves changed: Fig. 1 shows, with

the example of the 10 spectra, that the  $I(V)$  curve, and hence the structure of a 30-Å film, was different from those of a 14-Å film. We will show below that the structure of the thicker film is a strained modification of hcp Co(11 $\bar{2}$ 0).

The intensity data collected for QLEED analysis are considered more reliable for the  $1 \times 1$  films than for the  $c(2 \times 2)$  films because the quality of the LEED pattern was fairly good for the former, but poor for the latter. Nevertheless, both data yield interesting quantitative information about the atomic structure of, and the strains in, the Co films. In both cases, the thicknesses of the Co films analyzed below (14 and 30 Å, respectively) were larger than the penetration depth of the incident electrons [as confirmed by the stability of the  $I(V)$  curves], so that the films could be considered semi-infinite for the purposes of QLEED analysis.

### III. QLEED INTENSITY ANALYSES

The intensity calculations were performed with Jepsen's full-dynamical CHANGE program<sup>6</sup> and the following non-structural parameters: a Co potential taken from the collection of Moruzzi, Janak, and Williams;<sup>7</sup> 8 phase shifts and 61 beams up to 360 eV; an inner potential  $V_0 = -(10 + 4i) \text{ eV}$ , with the real part adjustable in the fitting process [it became  $-(8 \pm 3) \text{ eV}$  after refinement]; and an isotropic root-mean-square amplitude of thermal vibrations of  $0.15 \text{ \AA}$ . Evaluation of the agreement between theoretical and experimental curves was done both by  $R$ -factor analysis and visually. Three  $R$  factors were used, namely, the Van Hove–Tong  $R_{\text{VHT}}$ <sup>8</sup> the Zanazzi–Jona  $r_{\text{ZJ}}$ ,<sup>9</sup> and the Pendry  $R_p$  (Ref. 10) factors.

#### A. Analysis of the $1 \times 1$ Co film

The intensity calculations assumed as a model a semi-infinite Co crystal with an in-plane lattice constant equal to that of Fe, namely,  $2.866 \text{ \AA}$ , as required by the observed pseudomorphism. In the calculations, both the bulk interlayer spacing  $d_{\text{bulk}}$  and the first interlayer spacing  $d_{12}$ , respectively, were varied:  $d_{\text{bulk}}$  from  $1.10$  to  $1.42 \text{ \AA}$  in steps of  $0.02 \text{ \AA}$  and the change  $\Delta d_{12}$  of  $d_{12}$  from  $-0.2$  to  $+0.2 \text{ \AA}$  in steps of  $0.05 \text{ \AA}$ . For the 14-Å Co film, both the visual evaluation, on the one hand, and the three  $R$  factors, on the other, found satisfactory agreement for

$$d_{\text{bulk}} = 1.396 \text{ \AA}, \quad \Delta d_{12} = -0.15 \text{ \AA},$$

with precision of the order of  $0.005 \text{ \AA}$  and accuracy estimated at  $\pm 0.03 \text{ \AA}$ . Contour plots of the three  $R$  factors used are depicted in Fig. 2: the minimum values are  $R_{\text{VHT}} = 0.28$ ,  $r_{\text{ZJ}} = 0.14$ , and  $R_p = 0.43$ . The calculated  $I(V)$  curves are compared to the experimental ones in Fig. 3.

#### B. Analysis of the $c(2 \times 2)$ Co film

The observations made in the present case are similar to those made in the case of Co on FeAl{001}.<sup>5,11</sup> In that case, the tendency of Co to revert to its stable phase (the hcp phase) was favored by the relatively small mismatch between the rectangular net of hcp Co(11 $\bar{2}$ 0) and the square net of FeAl{001}. In the present case, a similar phenomenon may occur owing to the relatively small mismatch between hcp Co(11 $\bar{2}$ 0) and Fe{001}.

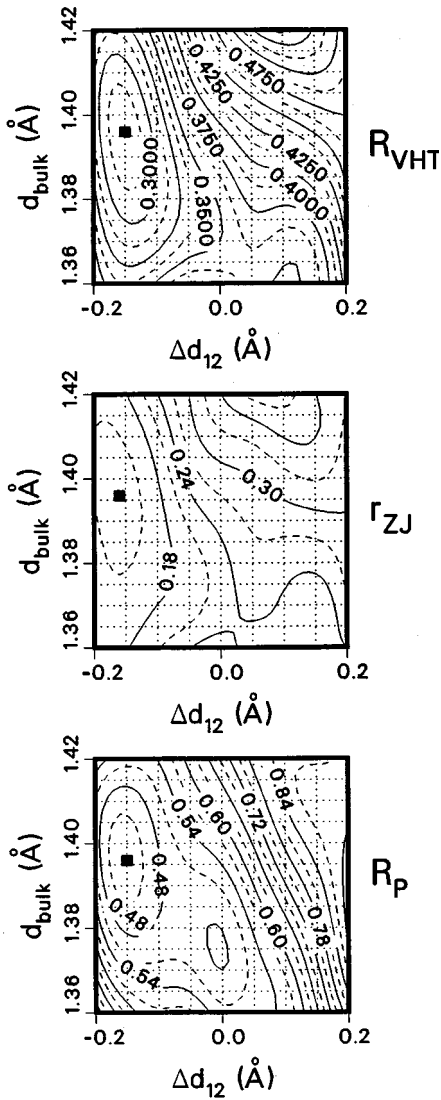


FIG. 2. Contour plots of the three  $R$  factors used in this study in the  $d_{\text{bulk}}$  versus  $\Delta d_{12}$  plane. All three  $R$  factors have minima at  $d_{\text{bulk}}=1.396 \text{ \AA}$  and  $\Delta d_{12}$  between  $-0.15$  and  $-0.16 \text{ \AA}$ .

Figure 4 depicts the respective unit meshes to scale. The primitive unit mesh of Fe{001} ( $2.866 \text{ \AA}$  on the side) has diagonals  $4.053 \text{ \AA}$  long, so that the {001} net may be described by the centered square with sides  $4.053 \text{ \AA}$  (top drawing in Fig. 4). The lattice parameters of hcp Co are  $a=2.507 \text{ \AA}$  and  $c=4.070 \text{ \AA}$ , hence the unit mesh of hcp Co(11 $\bar{2}$ 0) is a rectangle with a basis: the sides are  $4.342 \text{ \AA}$  ( $=2 \times a \times \sin 60^\circ$ ) and  $4.070 \text{ \AA}$  ( $=c$ ), respectively, and the second basis atom is located halfway along the  $c$  axis,  $1.447 \text{ \AA}$  ( $=\frac{4.342}{3}$ ) away from the shorter edge of the rectangle (bottom drawing in Fig. 4). A 6.64% compression of the  $4.342\text{-\AA}$  side to  $4.053 \text{ \AA}$  and a 0.40% compression of the  $4.070\text{-\AA}$  side to  $4.053 \text{ \AA}$  would fit the hcp Co(11 $\bar{2}$ 0) net onto the bcc Fe{001} net. The (11 $\bar{2}$ 0) net would have to be rotated  $45^\circ$  with respect to the (100) directions of the cubic {001} net, which would explain the occurrence of the  $c(2 \times 2)$  pattern. The relative orientations of the two nets can be seen in Fig. 2 of Ref. 11.

To prove that this kind of epitaxial growth occurs in the present case we must carry out a QLEED intensity analysis. As mentioned above, intensity data could be obtained from

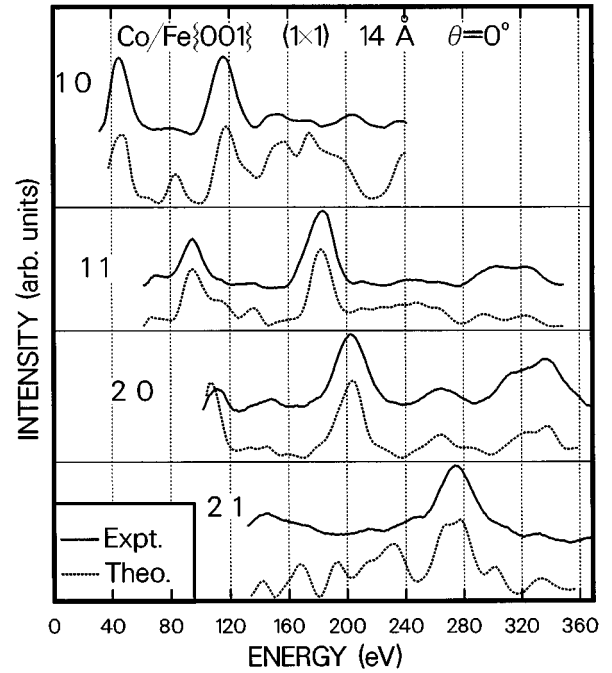


FIG. 3. Normal-incidence experimental (solid) and theoretical (dotted) LEED spectra from a  $14\text{-\AA}$  Co film grown on Fe{001}. The structure of the film is body-centered tetragonal (see the text).

the  $c(2 \times 2)$  film (about  $30 \text{ \AA}$  thick) despite the fact that the background was very high and the diffracted beams very broad. The calculations were done for four different values of  $d_{\text{bulk}}$  ( $1.27, 1.29, 1.31,$  and  $1.33 \text{ \AA}$ ) in each case varying  $\Delta d_{12}$  from  $-0.2$  to  $+0.2 \text{ \AA}$  in steps of  $0.05 \text{ \AA}$ . Note that the calculations were done for a single chosen orientation of the strained hcp (11 $\bar{2}$ 0) net with respect to the cubic {001} net and were then averaged over the four orientations possible in order to establish the fourfold symmetry detected experimentally. Also, the calculated beams, indexed on the hcp net, had to be reindexed on the cubic net in order to match the proper experimental beams. The relations are explained in detail for the case of Co on FeAl{001} in Ref. 11.

The best fit to the available experimental data was achieved with the parameters

$$d_{\text{bulk}}=1.29 \pm 0.03 \text{ \AA}, \quad \Delta d_{12}=-0.13 \pm 0.03 \text{ \AA},$$

with  $R$ -factor values  $R_{\text{VHT}}=0.33$ ,  $r_{\text{ZJ}}=0.13$ , and  $R_P=0.15$ . Calculated and observed  $I(V)$  curves are compared to one another in Fig. 5: the agreement is considered to be satisfactory in view of the poor quality of the LEED pattern observed.

#### IV. STRAIN ANALYSIS

The QLEED intensity analysis of the  $1 \times 1$  Co film shows it to have a body-centered-tetragonal structure with  $a=2.866 \text{ \AA}$  and  $c=2 \times 1.396=2.79 \text{ \AA}$ . To prove that this structure results from a distortion of bcc Co (as opposed to a distortion of fcc Co) due to the epitaxial strain on Fe{001}, we must carry out a strain analysis. We have shown elsewhere (see, e.g., Ref. 12) that an equilibrium (i.e., unstrained) cubic phase with lattice constant  $a_{\text{eq}}$  and interlayer spacing  $d_{\text{eq}}$ , growing pseudomorphically on a cubic {001} substrate with

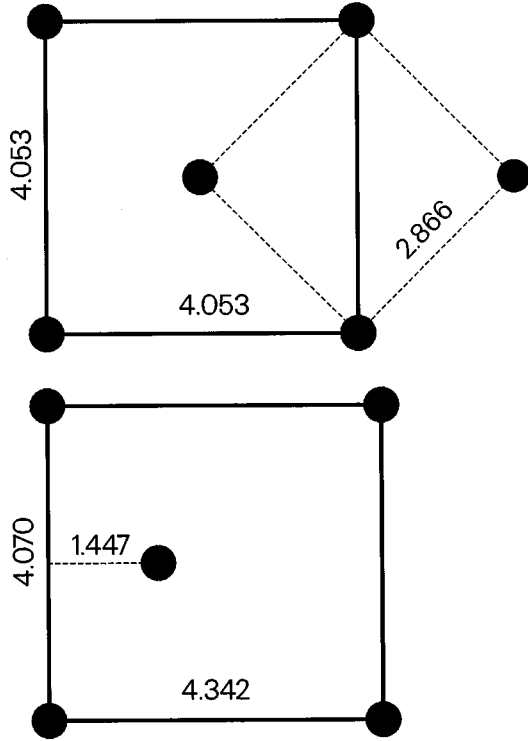


FIG. 4. Top: face-centered (solid lines) and primitive (dashed lines) meshes of Fe{001}. Bottom: unit mesh of hcp Co(1120). All numbers are in angstroms and the meshes are drawn to scale. In Co/Fe{001} films thicker than about 15 Å, the rectangular unit mesh of Co(1120) is forced to fit onto the centered square of Co{001} pseudomorphic with Fe{001}.

in-plane lattice constant  $a$ , will be tetragonally distorted to assume an interlayer spacing  $d$  determined by

$$\frac{d}{d_{\text{eq}}} = \left( \frac{a}{a_{\text{eq}}} \right)^{-\gamma}, \quad (1)$$

where  $\gamma = 2c_{12}/c_{11}$  and the  $c_{ik}$  are elastic constants of the equilibrium phase. Thus, if we know the equilibrium phase and its elastic constants we can calculate  $d$  from Eq. (1) and compare it with the value of  $d_{\text{bulk}}$  measured experimentally with QLEED.

Assume first that the equilibrium phase of the  $1 \times 1$  Co films grown in this work is the fcc phase, which has a lattice constant  $a_0 = 3.544$  Å, so that the primitive unit mesh is a square with sides  $a_{\text{eq}} = 2.506$  Å, while  $d_{\text{eq}} = 1.772$  Å. The elastic constants of fcc Co are  $c_{11} = 2.52$ ,  $c_{12} = 1.6$ , and  $c_{44} = 1.28$ , all in units of  $10^{12}$  dyn/cm<sup>2</sup>.<sup>13</sup> Hence, with  $a = 2.866$  Å we calculate from Eq. (1) that  $d = 1.484$  Å, which is outside the  $\pm 0.03$ -Å estimated experimental error of the value determined above,  $d_{\text{bulk}} = 1.396$  Å, and therefore disqualifies fcc Co as the equilibrium phase.

Assume then that the equilibrium phase is bcc Co, for which  $a_{\text{eq}} = 2.83$  Å (Ref. 14) and hence  $d_{\text{eq}} = 1.415$  Å. The elastic constants of bcc Co have not been measured, but they can be estimated from first-principles calculations of the shear modulus  $G$  (Ref. 15) and the bulk modulus  $B$  (Ref. 16) to be  $c_{11} = 3.604$  and  $c_{12} = 1.752$  in units of  $10^{12}$  dyn/cm<sup>2</sup>. We calculate from Eq. (1) that in this case  $d = 1.398$  Å, in excellent agreement with the value 1.396 Å determined above.

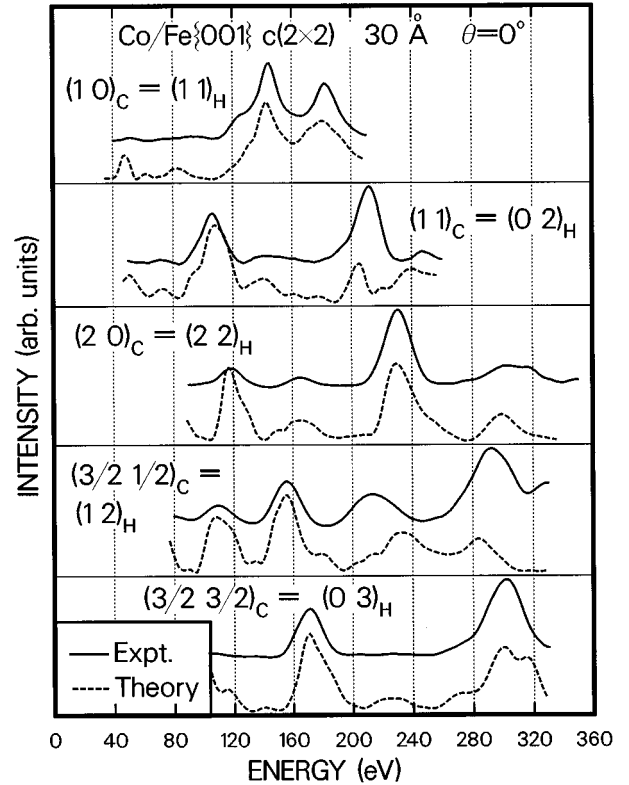


FIG. 5. Normal-incidence experimental (solid) and theoretical (dotted) LEED spectra from a 30-Å Co film grown on Fe{001} exhibiting a  $c(2 \times 2)$  LEED pattern. The spectra are identified both by their indexing on the cubic  $c(2 \times 2)$  pattern (subscript  $C$ ) and by their indexing on the hcp  $(11\bar{2}0)$  pattern (subscript  $H$ ). The relation between the two nets is explained in Ref. 11.

A convenient graphical representation of these results is given by means of the so-called epitaxial lines.<sup>17</sup> From Eq. (1) we calculate  $d$  for several assumed values of  $a$  (i.e., for different cubic {001} substrates) assuming either the fcc or the bcc phase as the equilibrium phase, and then we plot  $d$  versus  $a$  for both cases, getting a fcc epitaxial line and a bcc epitaxial line, as done in Fig. 6. This plot shows convincingly that the experimental result (open circle) fits well on the bcc line. For comparison, the QLEED result for  $1 \times 1$  Co films grown on FeAl{001} is also shown; in that case, as in the present case, the equilibrium phase is bcc Co.

## V. EFFECT OF OXYGEN

An unexpected effect of oxygen on the growth of Co on Fe{001} was found in the course of the present work. Deposition of Co onto the {001} surface of an iron crystal that contained large amounts of oxygen, but still produced a sharp  $1 \times 1$  LEED pattern, resulted in Co films that still exhibited  $1 \times 1$  LEED patterns even at thicknesses of about 30 Å [recall that on a clean Fe{001} surface the Co films converted from  $1 \times 1$  to  $c(2 \times 2)$  LEED patterns already at about 15 Å thickness]. The presence of oxygen in the surface layer of the substrate was revealed both by AES and by LEED. We show in Fig. 7 the 10 spectrum measured on a clean Fe{001} surface, the 10 spectrum measured on the {001} surface of the oxygen-rich Fe sample, and the 10 spectrum measured in Ref. 18(a) from an Fe{001} surface covered with a

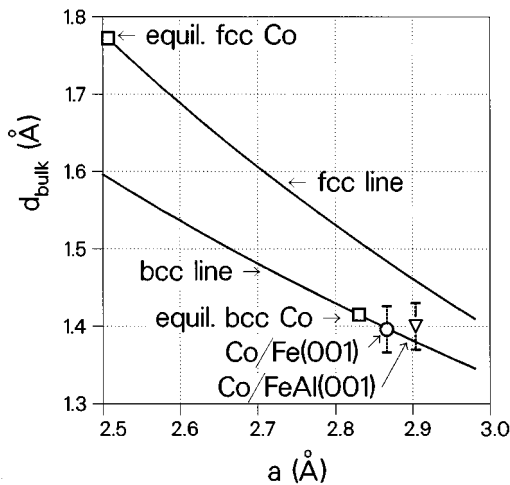


FIG. 6. Epitaxial lines for bcc and fcc Co in the  $d_{\text{bulk}}$  versus  $a$  plane. The circle and the triangle mark the experimental results of QLEED studies of Co/Fe{001} (this work) and of Co/FeAl{001} (Refs. 5 and 11). In both cases, it is obvious that the equilibrium phase of the strained Co films was, within the experimental error bars, the bcc phase.

monolayer of oxygen.<sup>18</sup> The agreement between the two latter curves (and others not shown) clearly demonstrates that the surface of the oxygen-rich sample was covered with an ordered monolayer of oxygen.

We then exposed a clean Fe{001} to oxygen gas to the point of obtaining a  $1 \times 1$  oxygen overlayer [a structure denoted Fe{001}  $1 \times 1$ -O (Ref. 18)] and then proceeded to deposit Co: the background of the LEED pattern increased considerably as the Co films grew thicker, but the structure remained clearly  $1 \times 1$  up to 30 Å (the largest thickness attained in this work). We collected  $I(V)$  curves from a 15-Å and a 30-Å Co film grown on Fe{001}  $1 \times 1$ -O and found them practically identical to one another. We then carried out QLEED intensity analyses for both sets of data by varying

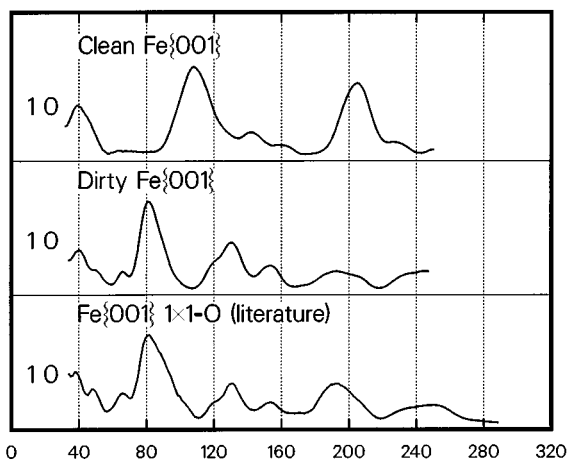


FIG. 7. Normal-incidence experimental 10 LEED spectra from a clean Fe{001} surface (top), the {001} surface of an oxygen-rich Fe crystal (middle), and the Fe{001} $1 \times 1$ -O structure (from Ref. 18) (bottom). The strong similarity between the middle and the bottom curve shows that the oxygen-rich Fe{001} sample was covered by an ordered  $1 \times 1$  monolayer of oxygen.

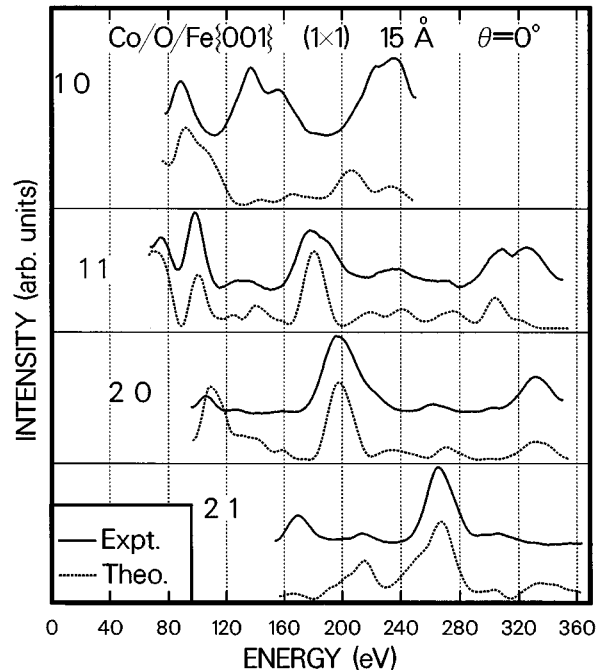


FIG. 8. Normal-incidence experimental (solid) and theoretical (dotted) LEED spectra from a 15-Å Co film grown on Fe{001} $1 \times 1$ -O.

the bulk interlayer distance  $d_{\text{bulk}}$  in the Co film, the O-Co interlayer distance  $d_{\text{O-Co}}$ , and the first Co-Co interlayer distance  $d_{\text{Co-Co}}$ . The results were then averaged to the values

$$d_{\text{bulk}} = 1.40 \pm 0.05 \text{ \AA}, \quad d_{\text{O-Co}} = 0.46 \pm 0.03 \text{ \AA},$$

$$d_{\text{Co-Co}} = 1.40 \pm 0.1 \text{ \AA}.$$

We compare in Fig. 8 the calculated curves to the 15-Å film data. The  $R$ -factor values are  $R_{\text{VHT}} = 0.37$ ,  $r_{\text{ZJ}} = 0.15$ , and  $R_p = 0.58$ . The fit is only mediocre, undoubtedly because of the poor quality of the LEED patterns. However, despite the presence of disorder in the film, we can reach with confidence the following conclusions: (i) the long-range-ordered regions in the Co films were pseudomorphic with the Fe substrate; (ii) their structure was essentially the same body-centered-tetragonal structure that the Co film assumed on clean Fe{001}; (iii) the films were covered by an ordered monolayer of oxygen (as also confirmed by AES data); (iv) but the transition to hcp (1120) (which occurred at a thickness of about 15 Å in the pure film) was suppressed, i.e., the range of stability of the strained bcc structure was extended to above 30 Å.

## VI. CONCLUSION

Ultrathin films of Co grown on clean Fe{001} with thicknesses up to about 15 Å are pseudomorphic with the substrate and have a body-centered-tetragonal (bct) structure with  $a = 2.866 \text{ \AA}$  and  $c = 2.792 \text{ \AA}$  and with an 11% contracted first interlayer spacing. This bulk bct structure is shown to be derived from strained bcc Co and not strained fcc Co in two ways. The known lattice constant and elastic constants of fcc Co yield a value  $d_{\text{bulk}}$  of the epitaxial film that disagrees with the measured  $d_{\text{bulk}}$  by an amount well outside the error esti-

mate, whereas the lattice constant and elastic constants of bcc Co obtained from experiment and theory yield a value of  $d_{\text{bulk}}$  in good agreement with the measured value. The strains are 1.3% in the two  $\langle 100 \rangle$  directions within and 1.4% in the direction perpendicular to the plane of the film. This growth is one more example of the commonly encountered case of epitaxy (so-called case 1) in which the unit mesh of the substrate and the unit mesh of the equilibrium phase of the film are geometrically similar to one another, i.e., they differ only in scale.

Thicker films of Co, up to about 30 Å thick, produce a  $c(2 \times 2)$  LEED pattern on high background, signaling large amounts of defects and disorder. The long-range-ordered regions of the films are found to have a strained hcp ( $11\bar{2}0$ ) structure: the strains are a 6.6% compression in one and a 0.4% compression in the other direction within the film plane and a 2.9% expansion in the direction perpendicular to it. This growth is an example of a rarer case of epitaxy (case 2) in which the unit meshes of substrate and film's equilibrium phase differ in lengths of the sides or angles between the sides or both.

The sequence of events in the present case is similar to that observed during the growth of Co on FeAl{001}.<sup>5,11</sup> The lattice constant of the FeAl sample used in that study was  $a=2.904$  Å, hence the mismatch to bcc Co ( $a=2.83$  Å, epitaxial strain of 2.6%) was larger than the mismatch to Fe ( $a=2.866$  Å, epitaxial strain 1.3%) and both involve expansions of the bcc Co unit mesh. Thus the Co{001} film is less strained on Fe{001} than on FeAl{001}.

The opposite is true for the hcp ( $11\bar{2}0$ ) film. On FeAl{001}, the Co film is compressed by 5.4% in one direction and expanded by 0.91% in the other direction within the plane of the film and expanded by 2.9% in the direction perpendicular to it. On Fe{001}, the hcp ( $11\bar{2}0$ ) film is compressed by 6.6% in one and compressed by 0.4% in the other in-plane direction and expanded by 2.9% in the perpendicular direction. This fact may explain why the corresponding  $c(2 \times 2)$  LEED patterns were much better on the FeAl{001} substrate than on the Fe{001} substrate. In both cases, it is noteworthy that the strained hcp ( $11\bar{2}0$ ) film does not grow directly onto the substrate (although the geometrical relation-

ships are the same as later on in the growth), but starts only after about ten layers of strained bcc Co have been deposited. We cannot tell whether the strained hcp ( $11\bar{2}0$ ) film grows on top of the strained bcc {001} film or whether the latter converts to the strained hcp ( $11\bar{2}0$ ) structure when the critical thickness of about 15 Å is reached. We consider the conversion unlikely, because in that case the  $c(2 \times 2)$  structure would appear to be well developed soon after the critical thickness is reached, whereas the observations show that the  $c(2 \times 2)$  structure develops slowly with increasing thickness and becomes distinguishable over the high background when the film thickness has reached about 30 Å.

The present results are in good semiquantitative agreement with the work of Houdy *et al.*,<sup>3</sup> despite the differences in experimental conditions. Houdy *et al.* grew Fe/Co multilayers, varying the thicknesses of the two types of films, by rf sputtering on Si{111} substrates. Presumably, at least portions of the films were epitaxial and pseudomorphic with {111} orientation, which may explain the observation of a "mixed hcp-fcc structure" of Co films thicker than about 20 Å (stacking faults in Co{111} films would change hcp to fcc and vice versa). The interesting point is that the existence of a critical thickness of the order of 15–20 Å beyond which the (strained and metastable) bcc phase gives way to the (strained but stable) hcp phase seems to be common to both {001} and {111} films, as well as to single- and multilayer structures.

The observed effect of oxygen on the growth of the Co film is interesting because it shows not only that the oxygen layer acts as a surfactant, in the sense that it "floats" on top of the growing film, but also that in its presence the critical thickness for the growth of the hcp ( $11\bar{2}0$ ) film is increased to beyond 30 Å. One may speculate that the oxygen layer could hold the Co layer underneath on a square net, resisting the tendency toward a rectangular net with a noncentered basis atom.

#### ACKNOWLEDGMENT

This work was sponsored in part by the National Science Foundation Grant No. DMR9404421.

<sup>1</sup>H. Li and B. P. Tonner, Phys. Rev. B **40**, 10 241 (1989).

<sup>2</sup>J. Zhang, Z.-L. Han, S. Varma, and B. P. Tonner, Surf. Sci. **298**, 351 (1993).

<sup>3</sup>Ph. Houdy, P. Boher, F. Giron, F. Pierre, G. Chappert, P. Beauvillain, K. Le Dang, P. Veillet, and E. Velu, J. Appl. Phys. **69**, 5667 (1991).

<sup>4</sup>F. Jona, J. A. Strozier, Jr., and P. M. Marcus, in *The Structure of Surfaces*, edited by M. A. Van Hove and S. Y. Tong (Springer-Verlag, Berlin, 1985), p. 92.

<sup>5</sup>C. P. Wang, S. C. Wu, F. Jona, and P. M. Marcus, Phys. Rev. B **49**, 17 385 (1994).

<sup>6</sup>D. W. Jepsen, Phys. Rev. B **22**, 814 (1980); **22**, 5701 (1980).

<sup>7</sup>V. L. Moruzzi, J. F. Janak, and A. R. Williams, *Calculated Electronic Properties of Metals* (Pergamon, New York, 1978).

<sup>8</sup>M. A. Van Hove, S. Y. Tong, and M. H. Elconin, Surf. Sci. **64**, 85 (1977).

<sup>9</sup>E. Zanazzi and F. Jona, Surf. Sci. **62**, 61 (1977).

<sup>10</sup>J. B. Pendry, J. Phys. C **13**, 937 (1980).

<sup>11</sup>C. P. Wang, S. C. Wu, F. Jona, and P. M. Marcus, Phys. Rev. B **49**, 17 391 (1994).

<sup>12</sup>P. M. Marcus and F. Jona, J. Phys. Chem. Solids **55**, 1513 (1994); Surf. Rev. Lett. (to be published).

<sup>13</sup>*Elastic, Piezoelectric, Pyroelectric, Piezooptic, Electrooptic Constants, and Nonlinear Dielectric Susceptibilities of Crystals*, edited by K.-H. Hellwege and A. M. Hellwege, Landolt-Börnstein, New Series, Group III, Vol. 18, (Springer-Verlag, Berlin, 1984), p. 3.

<sup>14</sup>G. A. Prinz, Phys. Rev. Lett. **54**, 1051 (1985); J. J. Krebs, Appl. Phys. A **49**, 513 (1989).

<sup>15</sup>T. Kraft, P. M. Marcus, and M. Scheffler (unpublished).

<sup>16</sup>V. L. Moruzzi and P. M. Marcus give theoretical lattice constants and bulk moduli for 3d and 4d transition elements in both bcc

and fcc structure in the *Handbook of Magnetic Materials*, edited by K. H. J. Buschow (Elsevier, New York, 1993), Vol. 7, Chap. 2.

<sup>17</sup>P. M. Marcus and F. Jona, *Phys. Rev. B* **51**, 17 081 (1995).

<sup>18</sup>(a) K. O. Legg, F. Jona, D. W. Jepsen, and P. M. Marcus, *Phys. Rev. B* **16**, 5271 (1977); (b) F. Jona and P. M. Marcus, *Solid State Commun.* **64**, 667 (1987).

<sup>19</sup>It may be worth mentioning here that the exposure reported in Ref. 18(a) as necessary to form a  $1\times 1$  oxygen adlayer (6–7 L [Ref. 18(a)]) was not sufficient to produce the same structure in

the present experiments. Achievement of the desired structure was tested by comparing the  $I(V)$  curves measured after exposure to oxygen gas with those published in Ref. 18(a), which, as mentioned above, are almost identical to those obtained in this work from the oxygen-rich Fe sample. The exposure needed here was initially about 750 L and decreased to about 500 L in the fourth experiment. The reasons for the difference between the present and the Ref. 18(a) exposures are not understood at this time.